ChemPubSoc Europe

DOI: 10.1002/open.201500124

Open Access ChemistryOPEN Full Papers

Application of Near-IR Absorption Porphyrin Dyes Derived from Click Chemistry as Third-Order Nonlinear Optical Materials

Yongsheng Mi,[a] Pengxia Liang,[a] Zhou Yang,*[a] Dong Wang,*[a] Hui Cao,[a] Wanli He,[a] Huai Yang,*[b] and Lian Yu*[c]

Recently, third-order nonlinear properties of porphyrins and porphyrin polymers and coordination compounds have been extensively studied in relation to their use in photomedicine and molecular photonics. A new functionalized porphyrin dye containing electron-rich alkynes was synthesized and further modified by formal [2+2] click reactions with click reagents tetracyanoethylene (TCNE) and 7, 7, 8, 8-tetracyanoquinodimethane (TCNQ). The photophysical properties of these porphyrin dyes, as well as the click reaction, were studied by UV/Vis spectroscopy. In particular, third-order nonlinear optical properties of the dyes, which showed typical D-π-A structures, were characterized by Z-scan techniques. In addition, the self-assembly properties were investigated through the phase-exchange method, and highly organized morphologies were observed by scanning electron microscopy (SEM). The effects of the click post-functionalization on the properties of the porphyrins were studied, and these functionalized porphyrin dyes represent an interesting set of candidates for optoelectronic device components.

Introduction

Materials with nonlinear optical (NLO) properties and fast response to laser irradiation, as well those as with merits such as small optical loss, high optical quality, good stability, low cost and ease of preparation, have attracted increasing attention owing to their potential applications in ultrafast optical switching, optical communication, optical modulators, and optical limiting.[1–5] The chemist's goal in this work is to design molecules and materials with high nonlinear coefficients and develop models that can predict these characteristics from the molecular structure.[6,7] Discovering organic molecules with large nonlinear responses is an active pursuit, and properties are often manipulated by making structural modifications to donor and acceptor building blocks, as well as to conjugated linking π-units.[8–10]

Porphyrins are comprised of four pyrrole units linked together through their α-positions by methane bridges; the highly delocalized aromatic 18π-electron system of porphyrins can give rise to a strong NLO response.[11] Recently, third-order NLO properties of porphyrins and porphyrin polymers and coordination compounds have been extensively studied in relation to their use in photomedicine and molecular photonics.[12–18]

Although continuous optimization was explored previously, some porphyrin derivatives were obtained through the fast, high-yielding, and catalyst-free [2+2] click reaction,[19] However, very little research has been done on the porphyrin dyes modified by [2+2] click chemistry with high third-order optical nonlinearities. In particular, innovative [2+2] cycloaddition of strong electron acceptors, such as tetracyanoethene (TCNE) and 7,7,8,8-tetracyanoquinodimethane (TCNQ), to electron-rich alkynes provides efficient access to nonplanar push–pull chromophores featuring intense intramolecular charge-transfer (CT) and optical properties.[20–22]

In this paper, we use click chemistry to aid the synthesis of extraordinary porphyrin derivatives, which provides the porphyrin derivatives with a widened absorption spectra and improved CT properties. These derivatives had D-π-A systems that contain a middle acceptor and peripheral multi-donors in contrast to the conventional linear type of D-π-A compounds, and were prepared by quite short and high-yielding synthetic routes. It is expected that the concept reported here can be

[a] Y. Mi,[+] P. Liang,[+] Prof. Z. Yang, D. Wang, H. Cao, W. He
Department of Materials Science and Engineering
University of Science and Technology Beijing
30 Xueyuan Rd, Haidian, Beijing 100083 (P. R. China)
E-mail: yangz@ustb.edu.cn
wangdong@ustb.edu.cn

[b] Prof. H. Yang
Department of Materials Science and Engineering, Peking University
5 Yiheyuan Rd, Haidian, Beijing 100871 (P. R. China)
E-mail: yanghuai@pku.edu.cn

[c] Dr. L. Yu
State Key Laboratory of Coal Resource and Safe Mining
China University of Mining & Technology
11 Xueyuan Rd, Beijing, (P. R. China)
E-mail: yulian4228@126.com

[+] The authors Y. Mi and P. Liang have contributed equally to this article.

Supporting information for this article is available on the WWW under http://dx.doi.org/10.1002/open.201500124.

expanded to other functional groups and may impact optoelectronic applications in the future.

Results and Discussion

Design and synthesis

A new ethynyl-bridged porphyrin intermediate (named **Por–Zn–N**) was designed and synthesized on the basis of Sonogashira coupling reactions (Scheme 1). Hence, alkynylpyrene derivative **Por–Zn–N**, which consisted of porphyrin as acceptor, *N*,*N*-didodecyl aniline as donor, and an ethynyl group as a bridge, was firstly prepared as a click precursor. The alkoxy groups were added in order to improve solubility and decrease aggregations of the porphyrin derivatives. The products were obtained in high yields, and these porphyrin derivatives have good solubility in dichloromethane and tetrahydrofuran (THF).

Click chemistry provides efficient, reliable, and selective reactions for synthesizing new compounds and generating combinatorial libraries. In particular, typically thermal [2+2] cycloadditions by reacting "electronically confused" alkynes with TCNE and TCNQ are considered to be novel examples. These *meso*-extended tetraarylporphyrin chromophores **PY–Zn–TCNE** and **PY–Zn–TCNQ** were obtained through the high-yielding [2+2] click reactions between alkynes and TCNE and TCNQ as shown in Scheme 2. The structures and purities of newly prepared products were confirmed by ^{1}H NMR, Fourier-transform infrared (FT-IR), and mass spectrometry.

The reactions with the click reagent TCNE could be conducted under ambient temperature, and enhancement of temperature to 100 °C was just for higher efficiency. However, the click reactions of TCNQ required heating up to 100 °C and holding at reflux for 1 h to generate significantly high yields ranging 96 %. Furthermore, in all click reactions, metal catalysts were unnecessary, and purifications were done more easily in contrast with other reactions for the absence of by-products. Moreover, the porphyrin derivatives were stable in the air at room temperature, and could be dissolved in common organic solvents such as dichloromethane, THF, and acetone, which were beneficial for further processing.

Photophysical properties

The photophysical properties of organic materials are essential parameters that provide important information on their conformations and electronic structures. The UV/Vis absorption properties of **Por–Zn–N**, **Por–Zn–TCNE**, and **Por–Zn–TCNQ** were characterized by UV/Vis spectroscopy in dilute dichloromethane solutions at 298 K, as shown in Figure 1. The UV/Vis spectra of these compounds exhibit features typical of a porphyrin ring, with an intense Soret band in the range 400–500 nm and less intense Q bands in the range 600–1200 nm.

It is worth noting that the strongest absorption peaks of both **Por–Zn–TCNE** (433 nm) and **Por–Zn–TCNQ** (453 nm) showed an obvious blue-shift relative to **Por–Zn–N** (474 nm), which was attributed to the cyano group as strong acceptors decrease the electronic cloud density of the porphine ring.[23] Meanwhile, **Por–Zn–TCNQ** is red shifted by 20 nm compared

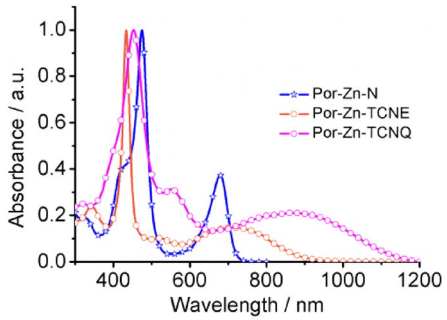

Figure 1. UV/Vis absorption spectra of **Por–Zn–N**, **Por–Zn–TCNE**, and **Por–Zn–TCNQ** in CH_2Cl_2 solutions.

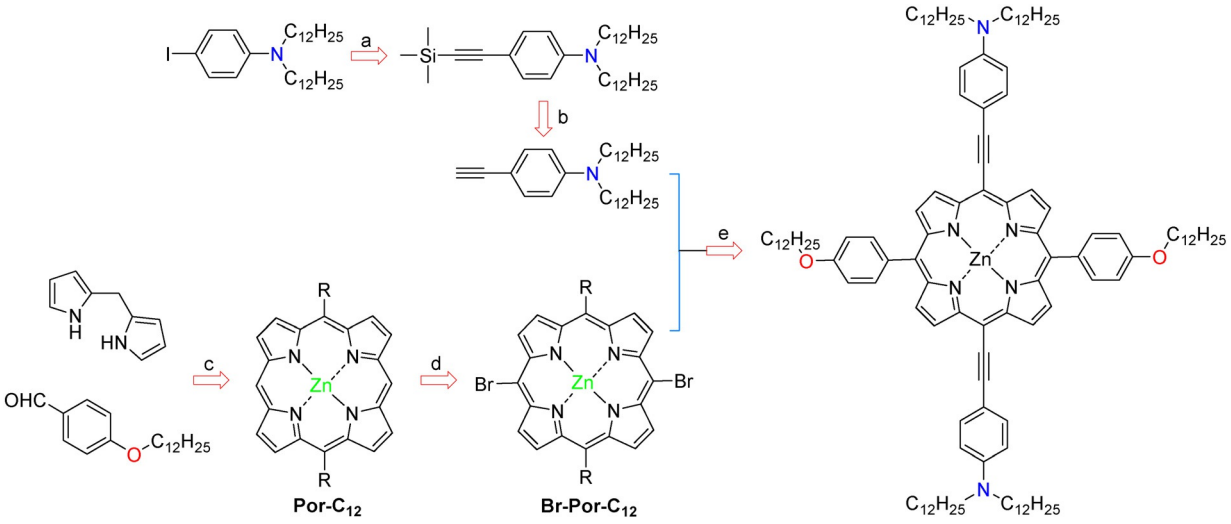

Scheme 1. Molecular structures and synthetic routes of **Por–Zn–N**. *Reagents and conditions*: a) trimethylsilylacetylene (TMSA), THF, Et_3N, $PdCl_2(PPh_3)_2$, CuI, 30 °C, 8 h, 13 %; b) K_2CO_3, MeOH, rt, 4 h, 93 %; c) 1) pyrrole, TFA, CH_2Cl_2, rt, 20 h, 2) $Zn(OAc)_2$, 93 %; d) NBS, CH_2Cl_2, rt, 1 h, 82 %; e) $Pd(PPh_3)_2Cl_2$, PPh_3, CuI, THF, Et_3N, 80 °C, 12 h, 83 %.

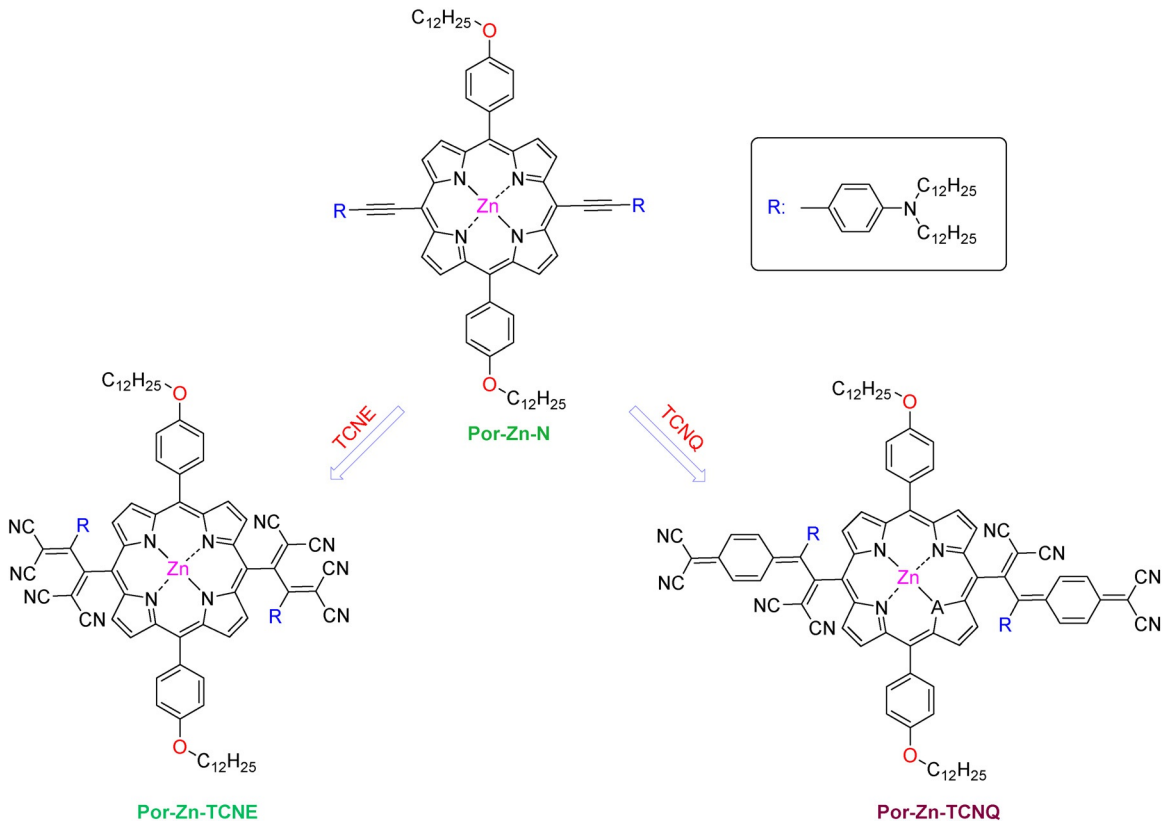

Scheme 2. Molecular structures and synthetic routes of the click reaction products.

with **Por**–**Zn**–**TCNE**, resulting from the effective π-extended conjugation caused by the hexatomic rings.

In comparison with **Por**–**Zn**–**N**, both clicked products showed end absorptions (λ_{end}) reaching into the near infrared (900 nm for **Por**–**Zn**–**TCNE** and 1200 nm for **Por**–**Zn**–**TCNQ**) which was ascribed to the electronic effect between the donor (porphyrin) and acceptor (cyano group). Another fact worth mentioning is that the λ_{end} of the products also showed obviously bathochromic shifts between **Por**–**Zn**–**TCNE** and **Por**–**Zn**–**TCNQ**, concomitantly with increased conjugation lengths.

Time-resolved transient absorption spectra of porphyrins in dichloromethane at room temperature were taken at various delay times after the excitation pulse. The spectral trace of **Por**–**Zn**–**N** is shown in Figure 2, which displays broad negative signals in the range of 400–500 nm and 630–700 nm, corresponding to the bleaching of the strongly allowed $S_0 \rightarrow S_n$ absorption band upon excitation and also shows a buildup of a strong transient absorption signals in the region of 500–600 nm. The latter peak was associated with the $S_1 \rightarrow S_n$ transition.[24,25] Compared with **Por**–**Zn**–**N**, the click products **Por**–**Zn**–**TCNE** and **Por**–**Zn**–**TCNQ** didn't show any signals under the same conditions, which were due to the increments of π-conjugations and introduction of electron-withdrawing cyano groups.

Hereafter, the reaction of **Por**–**Zn**–**N** was initially investigated by UV/Vis spectroscopic titration experiments by adding the click reagent TCNE in chlorinated solvents. As shown in Figure 3, Soret bands blue-shifted to 400–450 nm and increased with the increasing amount of the TCNE, finally leading to completely reddish-brown solutions. The presence of the isosbestic points at 410, 451, and 512 nm for **Por**–**Zn**–**N** indicated no side reactions during the TCNE click reaction. The position of the charge-transfer (CT) bands (at 437 nm) was obviously blue-shifted compared with the precursor **Por**–**Zn**–**N** (at 479 nm) during the experiments, suggesting that the electronic cloud density of porphyrin ring was decreased by the introducing of strong electron-withdrawing groups (cyano group). Porphyrin derivative **Por**–**Zn**–**N** displayed a significantly advantages that the products featured strong CT interactions in the visible absorption-region-related properties. Furthermore, the controlled introduction of these click products

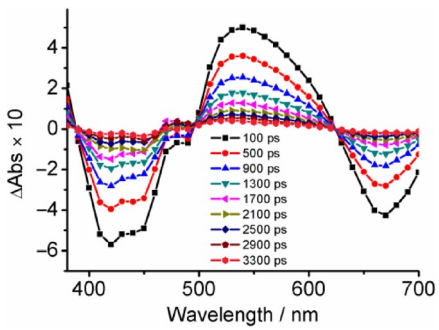

Figure 2. Picosecond time-resolved transient spectra of compound **Por**–**Zn**–**N** excited at 532 nm.

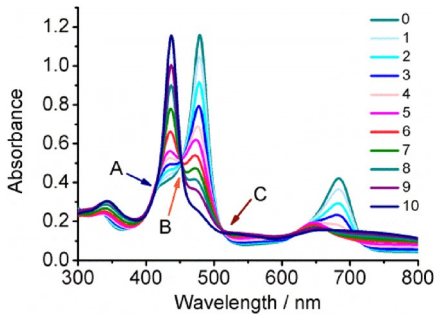

Figure 3. UV/Vis spectral changes of **Por**–**Zn**–**N** upon titration with TCNE (0–1.0 equiv) in dichlorobenzene at 20 °C.

into porphyrin was useful for optimization of the electronic states, thereby leading to the enhanced performance of various properties of optoelectronic materials. If the side-chain chromophores did not interact with each other, the peak top values should be constant. This result suggested that this click-type reaction could affect the electronic states of the whole conjugated compounds, and thus could be employed for tuning the energy levels of the conjugated materials.

Nonlinear optical (NLO) properties

The NLO properties corresponding to **Por**–**Zn**–**N**, **Por**–**Zn**–**TCNE**, and **Por**–**Zn**–**TCNQ** were measured by means of the Z-scan technique, of which several recordings were acquired. All of the samples were measured at 10^{-6} M solution in THF (spectral pure, SP), and the solvent itself did not show any third-order nonlinearities under the experimental conditions. The nonlinear absorption coefficient β and the nonlinear reflective index n_2 would be available under measurements, and the third-order nonlinear susceptibility could be calculated (detailed calculation methods are listed in the Supporting Information).

Figure 4 shows the "open-aperture" Z-scan data and the normalized transmittance curves of all products, which could be fitted perfectly with respect to equations reported by references.[19] In Figure 4a,b, profound transmittance valleys can be seen around the focal plane, which was characteristic of reverse saturable absorption (RSA)-type behavior of **Por**–**Zn**–**N** and **Por**–**Zn**–**TCNE**. Materials showing RSA became more opaque on exposure to high photon fluxes due to the high absorption from the excited state, and this property has been exploited in the field of optical limiting for laser protection. However, Figure 4c shows a typical transmittance peak of compound **Por**–**Zn**–**TCNQ**, which exhibits saturable absorption (SA)-type behavior. It could be observed that compared with **Por**–**Zn**–**N** and **Por**–**TCNE**, **Por**–**Zn**–**TCNQ** clearly exhibited reverse saturable absorption–saturable absorption (RSA-SA) transition by click reaction with TCNQ. The reason for conversion from the RSA to SA phenomenon for **Por**–**Zn**–**TCNQ** is the threshold intensity[26] determined by the parameters such as absorption cross section and level lifetime, and the saturation intensity declined dramatically. Once the incident light intensity crossed the threshold intensity, conversion from RSA to SA happened.

From a plethora of recordings, the $Im\chi^{(3)}$ (the imagery parts of the third-order nonlinearities) value of **Por**–**Zn**–**N** was found to be 1.0×10^{-11} esu, which corresponds to a nonlinear absorption coefficient of $\beta=4.8\times10^{-10}$ m W^{-1}. The $Im\chi^{(3)}$ values of **Por**–**Zn**–**TCNE** and **Por**–**Zn**–**TCNQ** were 1.7×10^{-14} esu and 3.6×10^{-14} esu, while the nonlinear absorption coefficients β were 7.9×10^{-13} m W^{-1} and -1.7×10^{-13}, respectively. Comparing to other organic molecules measured by Z-scan, the third-order nonlinear values of our compounds were relatively good.[27,28]

"Closed-aperture" Z-scan data of **Por**–**Zn**–**N**, **Por**–**Zn**–**TCNE**, and **Por**–**Zn**–**TCNQ** are shown in Figure 5. In this figure, the

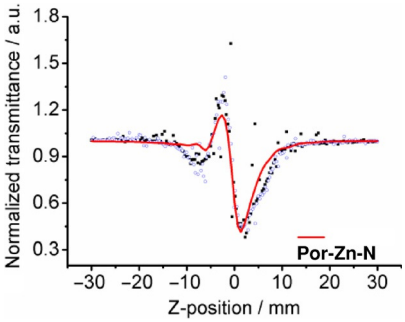

Figure 5. Closed-aperture Z-scans measured in the THF solution of **Por**–**Zn**–**N**.

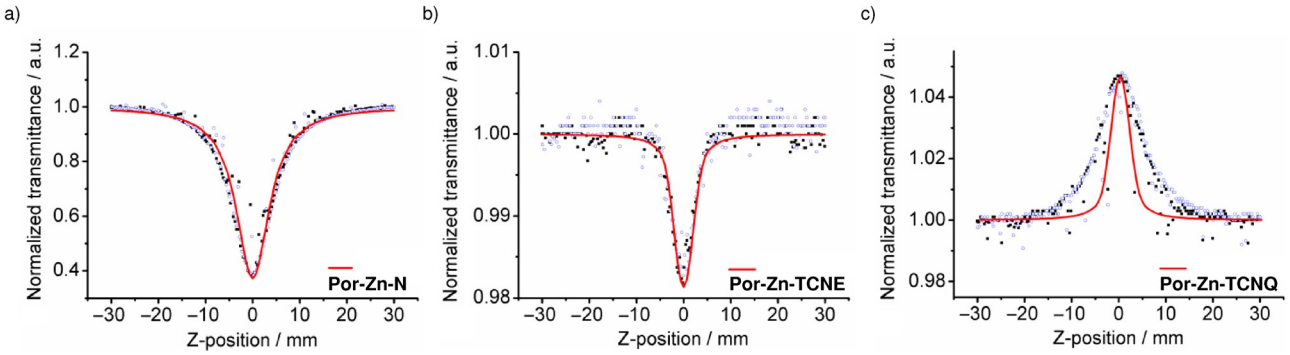

Figure 4. Open-aperture Z-scans measured in the THF solutions of a) **Por**–**Zn**–**N**, b) **Por**–**Zn**–**TCNE**, and c) **Por**–**Zn**–**TCNQ**.

normalized transmittance curve of **Por–Zn–N** could be fitted well according to the equation reported by reference and the real part of third-order nonlinearity, $Re\chi^{(3)}$, was found to be -1.1×10^{-11} esu, which corresponds to a nonlinear refractive index $n_2=-2.3\times10^{-17}$ m^2·w^{-1}. However, click products **Por–Zn–TCNE** and **Por–Zn–TCNQ** didn't show closed-aperture curves, and a plausible explanation could be that the nonlinear absorption is much stronger than the refraction. The properties of these products that we developed made it relatively important for new molecule synthesis used in NLO applications.

Self-assembly properties

To develop novel organic optoelectronic materials, the hierarchical self-assembly of multivalent components through the concerted action of multiple noncovalent interactions turns out to be one of the most promising approaches, as it allows the simultaneous organization of discrete molecules, long-range order, and inherently defect-free structures. Taking this into account, the introduction of an activated cyano group as acceptor and metal ions into the discoid porphyrin core could enhance multiple noncovalent interactions. The solvent-exchanging method was used to form regular self-assembly structures in the solution phase, and SEM images of self-assembled morphologies are shown in Figure 6. A discoid-distinct-like morphology shown in the Figure 6a was observed for compound **Por–Zn–N** because of the cooperation of the π–π interactions and the metal ions coupling between the layers (here mainly brickwork-type H-aggregates). The upper right corner of Figure 6a is a schematic diagram of molecular permutations of the discoid-distinct-like structure at the micron scale. By introducing click reagents TCNE and TCNQ substituents into the discoid cores, the degree of self-assembling order of the compounds was likely to worsen due to the increasing steric hindrance. Products **Por–Zn–TCNE** and **Por–Zn–TCNQ** did not exhibit regular discoid-distinct-like morphologies; rather, spherical morphologies as shown in Figure 6b,c.

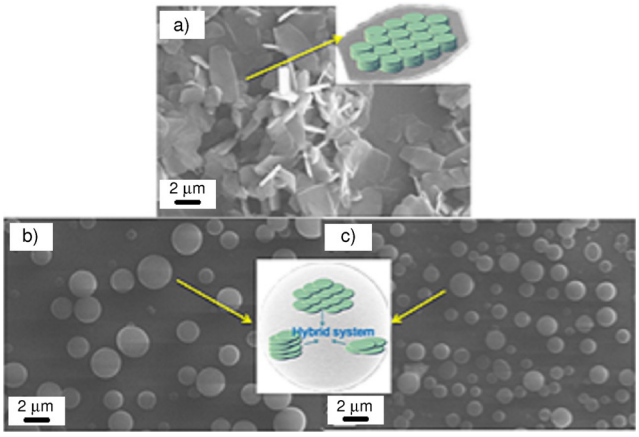

Figure 6. SEM images of self-assembled morphologies of compound a) **Por–Zn–N**, b) **Por–Zn–TCNE**, and c) **Por–Zn–TCNQ**; the yellow arrows are pointing to the aggregation mode of different self-assembling morphologies.

As the diagram shows, between Figure 6b and c, the morphologies could not be classified as pure J- or H-aggregates, but their combination. In addition, due to the greater steric hindrance effect, the size of the self-assembled spheres of **Por–Zn–TCNQ** was smaller than that of **Por–Zn–TCNE.** For most materials, J-aggregates of organic dyes are of significant interest for the development of advanced photonic technologies for their abilities to delocalize and migrate excitonic energy over a large number of aggregated dye molecules.[29]

Density functional theory (DFT) calculations

As shown in Figure 7, the DFT-optimized model structure of compound **Por–Zn–N** is close to planar. Both BP86 and TPSS calculations yielded similar results. According to the TPSS/RI/TZVP calculated results, the bond length of Zn–N is about 2.053 Å, and the four bond angles of N–Zn–N are 90.19. 89.88, 90.16, and 89.78°; the sum of four N–Zn–N angles is almost 360° (360.01°). Compared with the experimental results,[30] the bond length of Zn–N in compound ZnTPP is 2.045(2) Å, and the four bond angles are about 90.16, 80.84, 90.16, and 80.84°. The DFT-calculated results agreed well with the experimental data.

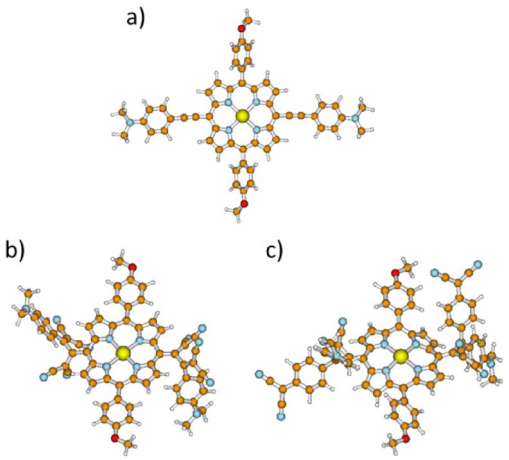

Figure 7. Optimized model structures obtained with DFT (TPSS/RI/TZVP) calculations for compounds a) **Por–Zn–N**, b) **Por–Zn–TCNE**, and c) **Por–Zn–TCNQ**. Zn atoms: yellow, N atoms: blue, O atoms: red, H atoms: white, C atoms: brown.

The DFT-optimized model structures of compounds **Por–Zn–TCNE** and **Por–Zn–TCNQ** are both crooked (bent) due to the large substituted groups introduced through click reactions with TCNE or TCNQ. As a result of these bent structures, spherical morphologies of compound **Por–Zn–TCNE** and **Por–Zn–TCNQ** could be observed by SEM (Figure 6)

Conclusion

In this work, a series of Zn-complexed D-π-A porphyrin derivatives, **Por–Zn–N**, **Por–Zn–TCNE**, and **Por–Zn–TCNQ** were designed and synthesized through [2+2] click reactions based on

the aniline groups as donor units and cyano groups as acceptor units. Investigations of the photophysical properties by using UV/Vis spectroscopy showed that the charge-transfer character of the D-π-A structures plays a key role in the absorption peak shifts, and the click products showed various bathochromic shifts. Most importantly, upon the introduction of electron acceptors by click reactions, the third-order nonlinear absorption of the products showed typical RSA-SA transition, and both the products revealed relatively good third-order nonlinear optical susceptibilities. In addition, the discoid-distinct-like and spherical morphologies were observed through a phase-exchange method for packing porphyrin molecules, and the results agreed well with DFT calculations. The structure–property relationships of these porphyrin derivatives were built and could help in promising applications in organic electronics.

Experimental Section

General conditions

Reagents were purchased from commercial sources (Aldrich) and used without further purification. Triethylamine (TEA) and THF were distilled and purged with Ar before use. TCNE and TCNQ were purchased from Aldrich, and all other reagents were purchased from commercial sources and used as received.

^{1}H NMR spectra of the samples were recorded with a Varian 400 MHz instrument (Palo Alto, CA, USA) in $CDCl_3$ using the residual solvent resonance of $CHCl_3$ at 7.26 ppm relative to $SiMe_4$ as internal reference. FT-IR spectra were recorded in KBr pellets using a PerkinElmer LR-64912C spectrophotometer (Waltham, MA, USA). Matrix-assisted laser desorption ionization time-of-flight mass spectra (MALDI-TOF-MS) were recorded on a Shimadzu AXIMA-CFR mass spectrometer (Kyoto, Japan). All UV/Visible spectra were recorded on a HITACHI U-3010 spectrophotometer (Tokyo, Japan). SEM images were obtained on a Jeol JSM-5400/LV (Tokyo, Japan) with accelerating voltage of 15 kV.

Synthesis

Synthesis of Por–C_{12}–Zn: To a degassed solution of dipyrromethane (146.0 mg, 1.00 mmol), 4-dodecyloxy-benzaldehyde (290.2 mg, 1.00 mmol) in CH_2Cl_2 (100 mL) was added trifluoroacetic acid (TFA, 0.60 mmol, 44 μL). The mixture was stirred in the dark for 3 h, and then 2,3-dichloro-5,6-dicyano-1,4-benzoquinone (DDQ, 0.90 mmol, 200.0 mg) was added. Afterwards, the solution was stirred at rt for another 1 h, and the solvent was removed under decreased pressure. The product was isolated by column chromatography (silica gel) using CH_2Cl_2/hexane 1:1 as eluent. Recrystalization from CH_2Cl_2/MeOH gave a red solid, **Por–C_{12}**, (0.065 mmol, 13%); ^{1}H NMR (400 MHz, $CDCl_3$): $\delta = 10.33$ (s, 2H), 9.42 (d, 4H, $J = 6.4$ Hz), 9.15 (d, 4H, $J = 6.4$ Hz), 8.20 (d, 4H, $J = 8.0$ Hz), 7.36 (d, 4H, $J = 6.4$ Hz), 7.29 (s, 2H,), 4.30 (t, 4H), 2.05 (m, 8H), 1.51 (m, 30H), 0.92 ppm (t, 6H); FT-IR (KBr): $\tilde{\nu} = 2920$, 2859, 1448, 1474, 1242, 784 cm^{-1}; MALDI-TOF-MS (dithranol) *m/z*: calcd for $C_{56}H_{70}N_4O_2$: 830.5, found: 830.7.

To a solution of **Por–C_{12}** (1.00 mmol) in CH_2Cl_2 (50 mL) was added a solution of $Zn(OAc)_2$ (283.0 mg, 1.29 mmol) in MeOH (10 mL). After the mixture was stirred at rt for 1 h, the solvent was removed under decreased pressure. The residue was extracted with CH_2Cl_2. The solvent was dried over anhydrous Na_2SO_4 and removed under decreased pressure. The product was recrystallized from CH_2Cl_2/MEOH to give a red solid **Por–C_{12}–Zn** (0.93 mmol, 93%);^{1}H NMR (400 MHz, $CDCl_3$): $\delta = 10.33$ (s, 2H), 9.42 (d, 4H, $J = 6.4$ Hz), 9.14 (d, 4H, $J = 6.4$ Hz), 8.20 (d, 4H, $J = 8.0$ Hz), 7.37 (d, 4H, $J = 6.4$ Hz), 4.31 (t, 4H), 2.04 (m, 8H), 1.68 (m, 8H), 1.55 (m, 24H), 0.93 ppm (t, 6H); FT-IR (KBr): $\tilde{\nu} = 2920$, 2859, 1449, 1474, 784 cm^{-1}; MALDI-TOF-MS (dithranol) *m/z*: calcd for $C_{56}H_{68}N_4O_2Zn$: 892.5, found: 892.3.

Synthesis of brominated porphyrin. To a solution of **Por–C_{12}–Zn** (1.00 mmol) in CH_2Cl_2 (100 mL) was added a solution of *N*-bromosuccinimide (NBS, 712.0 mg, 4.00 mmol) in CH_2Cl_2 (10 mL). After the mixture was stirred at rt for 1 h, the solvent was removed under decreased pressure. The brown solid product **Br–Por–C_{12}** was purified by column chromatography (silica gel) using CH_2Cl_2/hexane 1:1 as eluent (0.82 mmol, 82%);^{1}H NMR (400 MHz, $CDCl_3$): $\delta = 9.42$ (d, 4H, $J = 6.4$ Hz), 9.12 (d, 4H, $J = 6.4$ Hz), 8.22 (d, 4H, $J = 8.0$ Hz), 7.47 (d, 4H, $J = 6.4$ Hz), 4.28 (t, 4H), 2.06 (m, 8H), 1.66 (m, 8H), 1.45 (m, 24H), 0.93 ppm (t, 6H); FT-IR (KBr): $\tilde{\nu} = 2922$, 2859, 1508, 1448, 1242 and 788 cm^{-1}; MALDI-TOF-MS (dithranol) *m/z*: calcd for $C_{56}H_{66}Br_2N_4O_2$: 1048.3, found: 1048.2.

Hagihara–Sonogashira cross-coupling procedure. Synthesis of the **Por–Zn–N**: $Pd(PPh_3)_2Cl_2$ (17.0 mg, 0.0240 mmol), CuI (4.73 mg, 0.0240 mmol), and PPh_3 (16.2 mg, 0.0600 mmol) were added to a degassed solution of triethylamine (6 mL) and THF (10 mL) under Ar. Meanwhile **Br–Por–C_{12}** (0.556 g, 0.600 mmol) was added. While stirring, the reaction mixture was heated to 60 °C, and (4-ethynyl-phenyl)-dioctyl-amine (1.64 g, 4.80 mmol) was injected to get **Por–Zn–N**. After 15 min of stirring at this temperature, the reaction was heated to 80 °C and stirred o/n under Ar atmosphere. The cooled reaction mixture was diluted with CH_2Cl_2 and extracted with water. The organic phase was dried over $MgSO_4$, and the solvent was removed under decreased pressure. The crude product was purified by column chromatography (silica gel, petroleum ether) to afford the purple powder **Por–Zn–N** (0.871 g, 83%); ^{1}H NMR (400 MHz, $CDCl_3$): $\delta = 9.00$ (m, 8H), 8.11 (m, 8H), 7.29 (d, 4H, $J = 6.4$ Hz), 7.22 (d, 4H, $J = 6.4$ Hz), 4.28 (t, 4H), 3.36 (t, 8H), 2.01 (m, 16H), 1.65 (m, 16H), 1.52 (m, 32H), 1.40 (m, 36H) 1.34 (m, 32H), 0.94 ppm (m, 6H); FT-IR (KBr): $\tilde{\nu} = 2934$, 2182, 1668, 1522, 1245, 822 cm^{-1}; MALDI-TOF-MS (dithranol) *m/z* calcd for $C_{120}H_{174}N_6O_2Zn$ 1795.3, found 1795.7.

Synthesis of Por–Zn–TCNE. Compound **Por–Zn–N** (0.36 g, 0.20 mmol, 1 equiv) and TCNE (51.2 mg, 0.40 mmol, 2 equiv) were mixed in CH_2Cl_2 (10 mL). After stirring for 10 min, the solvent was removed under decreased pressure, and the crude product was purified by column chromatography (silica gel, ethyl acetate/petroleum ether 1:4) to give the final click-type reaction product **Por–Zn–TCNE** as a dark green solid (0.36 g, 89%); ^{1}H NMR (400 MHz, $CDCl_3$): $\delta = 7.52$ (12H, d, $J = 8.0$ Hz), 7.27 (2H, d, $J = 8.0$ Hz), 7.20 (4H, d, $J = 8.0$ Hz), 6.94 (4H, d, $J = 8.0$ Hz), 6.71 (4H, d, $J = 8.0$ Hz), 6.68 (2H, d, $J = 8.0$ Hz), 6.77 (2H, d, $J = 8.0$ Hz), 6.44 (2H, d, $J = 8.0$ Hz), 5.39 (2H, d, $J = 8.0$ Hz), 4.06 (4H, m), 3.78 (8H, m), 1.76–1.26 (120H, m), 0.88 ppm (18H, m); FT-IR (KBr): $\tilde{\nu} = 2923$, 2863, 2220, 1738, 1596, 1285, 1184 cm^{-1}; MALDI-TOF-MS (dithranol) *m/z*: calcd for $C_{132}H_{174}N_{14}O_2Zn$: 2051.3, found: 2049.6.

Synthesis of Por–Zn–TCNQ. Compound **Por–Zn–N** (0.36 g, 0.20 mmol, 1 equiv) and TCNQ (0.08 g, 0.40 mmol, 2 equiv) were dissolved in dichlorobenzene (10 mL). Under stirring, the reactor was heated to 140 °C and maintained for 1 h. The solvent of the cooled reaction mixture was removed under decreased pressure, and the crude product was purified by column chromatography (silica gel, ethyl acetate/petroleum ether = 1/4) to give the pure

Por–Zn–TCNQ as a black solid (0.38 g, 87%); ^{1}H NMR (400 MHz, $CDCl_3$): δ = 7.52 (12H, d, J = 8.0 Hz), 7.27 (2H, d, J = 8.0 Hz), 7.20 (4H, d, J = 8.0 Hz), 6.94 (4H, d, J = 8.0 Hz), 6.71 (4H, d, J = 8.0 Hz), 6.68 (2H, d, J = 8.0 Hz), 6.77 (2H, d, J = 8.0 Hz), 6.44 (2H, d, J = 8.0 Hz), 5.84 (8H, d, J = 8.0 Hz)5.39 (2H, d, J = 8.0 Hz), 4.06 (4H, m), 3.78 (8H, m), 1.76–1.26 (120H, m), 0.88 ppm (18H, m); FT-IR (KBr): $\tilde{\nu}$ = 2922, 2864, 2219, 1739, 1594, 1285, 1184, 980 cm^{-1}; MALDI-TOF-MS (dithranol) *m/z*: calcd for $C_{144}H_{182}N_{14}O_2Zn$: 2203.4, found: 2202.8.

Computational Methods

The all-electron Kohn–Sham DFT calculations were performed with the quantum-chemical program package TURBOMOLE.[31] The functional BP86[32–33] and TPSS[34] in combination with the resolution-of-the-identity ("RI") density fitting technique[35–36] and the TZVP basis sets[37] were applied in all the DFT calculations. All geometry optimizations were performed in *C1* symmetry. The molecular structures were visualized with the program Molden.[38]

Acknowledgements

This work was supported by the Major Project of International Cooperation of the Ministry of Science and Technology, China (Grant No. 2013DFB50340), the National Natural Science Foundation of China (Grant Nos. 51173017, 51373024, 51473020, and 61370048), the Beijing Higher Education Young Elite Teacher Project (Grant No. YETP0356), and the Fundamental Research Funds for the Central Universities (Grant No. FRF-TP-14-001A2).

Keywords: Click reactions · near-infrared absorption · porphyrin derivatives · self-assembly · third-order nonlinear optical properties

[1] Z. H. Shi, Y. S. Zhou, L. J. Zhang, C. C. Mu, H. Z. Ren, D. Hassan, D. Yang, H. M. Asif, *RSC Adv.* **2014**, *4*, 50277 – 50284.
[2] W. Bentoumi, J.-C. Mulatier, P.-A. Bouit, O. Maury, A. Barsella, J.-P. Vola, E. Chastaing, L. Divay, F. Soyer, P. Le Barny, Y. Bretonnière, C. Andraud, *Chem. Eur. J.* **2014**, *20*, 8909 – 8913.
[3] S. Barlow, J.-L. Brédas, Y. A. Getmanenko, R. L. Gieseking, J. M. Hales, H. Kim, S. R. Marder, J. W. Perry, C. Riskoa, Y. Zhang, *Mater. Horiz.* **2014**, *1*, 577 – 581.
[4] Q. D. Zheng, G. S. He, P. N. Prasad, *Chem. Phys. Lett.* **2009**, *475*, 250 – 255.
[5] K. Sanusi, S. Khene, T. Nyokong, *Opt. Mater.* **2014**, *37*, 572 – 582.
[6] J. Humphrey, D. Kuciauskas, *J. Phys. Chem. B* **2004**, *108*, 12016 – 12023.
[7] K. E. Sekhosana, T. Nyokong, *Opt. Mater.* **2014**, *37*, 139 – 146.
[8] S. Keinan, M. J. Therien, D. N. Beratan, W. T. Yang, *J Phys Chem. A* **2008**, *112*, 12203 – 12207.
[9] *Quadratic Nonlinear Optics in Poled Polymer Films: From Physics to Device* (Ed.: J. Zyss), Academic Press, San Diego, CA, **1994**.
[10] *Nonlinear Optical Materials* (Eds.: S. P. Karna, A. T. Yeates), ACS Symposium Series 628, American Chemical Society, Washington, DC, **1996**.
[11] M. O. Senge, M. Fazekas, E. G. A. Notaras, W. J. Blau, M. Zawadzka, O. B. Locos, E. M. N. Mhuircheartaigh, *Adv. Mater.* **2007**, *19*, 2737 – 2774.
[12] S. M. Kuebler, R. G. Denning, H. L. Anderson, *J. Am. Chem. Soc.* **2000**, *122*, 339 – 347.
[13] H. Kano, T. Kobayashi, *Opt. Commun.* **2000**, *178*, 133 – 139.
[14] T. E. O. Screen, J. R. G. Thorne, R. G. Denning, D. G. Bucknell, H. L. Anderson, *J. Am. Chem. Soc.* **2002**, *124*, 9712 – 9713.
[15] K. Ogawa, T. Q. Zhang, K. Yoshihara, Y. Kobuke, *J. Am. Chem. Soc.* **2002**, *124*, 22 – 23.
[16] M. Drobizhev, A. Karotki, M. Kruk, N. Z. Mamardashvili, A. Rebane, *Chem. Phys. Lett.* **2002**, *361*, 504 – 512.
[17] A. Karotki, M. Drobizhev, M. Kruk, C. Spangler, E. Nickel, N. Mamardashvili, A. Rebane, *J. Opt. Soc. Am. B* **2003**, *20*, 321 – 332.
[18] K. Ogawa, A. Ohashi, Y. Kobuke, K. Kamada, K. Ohta, *J. Am. Chem. Soc.* **2003**, *125*, 13356 – 13357.
[19] L. Pengxia, Z. Du, D. Wang, Z. Yang, H. Sheng, S. Liang, H. Cao, W. He, H. Yang, *ChemPhysChem* **2014**, *15*, 3523 – 3529.
[20] Z. K. Jin, D. Wang, X. K. Wang, P. X. Liang, Y. S. Mi, H. Yang, *Tetrahedron Lett.* **2013**, *54*, 4859 – 4864.
[21] T. Michinobu, J. C. May, J. H. Lim, C. Boudon, J. P. Gisselbrech, P. Seiler, M. Gross, I. Biaggio, F. Diederich, *Chem. Commun.* **2005**, 737 – 739.
[22] M. Kivala, C. Boudon, J. P. Gisselbrecht, P. Seiler, M. Gross, F. Diederich, *Chem. Commun.* **2007**, 4731 – 4733.
[23] P. D. Jarowski, Y. L. Wu, C. Boudon, J. P. Gisselbrecht, M. Gross, W. B. Schweizer, F. Diederich, *Org. Biomol. Chem.* **2009**, *7*, 1312 – 1322.
[24] J. Petersson, J. Henderson, A. Brown, L. Hammarström, C. P. Kubiak, *J. Phys. Chem. C* **2015**, *119*, 4479 – 4487.
[25] D. M. Niedzwiedzki, J. O. Sullivan, T. Polívka, R. R. Birge, H. A. Frank, *J. Phys. Chem. B* **2006**, *110*, 22872 – 22885.
[26] L. Jiang, F. S. Lu, Q. Chang, Y. Liu, H. B. Liu, Y. L. Li, W. Xu, G. L. Cui, J. P. Zhuang, X. F. Li, S. Wang, Y. L. Song, D. B. Zhu, *ChemPhysChem* **2005**, *6*, 481 – 486.
[27] X. Q. Zheng, M. Feng, Z. G. Li, Y. L. Song, H. B. Zhan, *J. Mater. Chem. C* **2014**, *2*, 4121 – 4122.
[28] A. Faccinetto, S. Mazzucato, D. Pedron, R. Bozio, S. Destri, W. Porzio, *ChemPhysChem* **2008**, *9*, 2028 – 2034.
[29] M. Supur, Y. Yamada, M. E. El-Khouly, T. Honda, S. Fukuzumi, *J. Phys. Chem. C* **2011**, *115*, 15040 – 15047.
[30] W. Robert Scheidt, J. U. Mondal, C. W. Eigenbrot, A. Adler, L. J. Radonovich, J. L. Hoard, *Inorg. Chem.* **1986**, *25*, 795 – 799.
[31] R. Ahlrichs, M. Bär, M. Häser, H. Horn, C. Kölmel, *Chem. Phys. Lett.* **1989**, *162*, 165 – 169.
[32] A. D. Becke, *Phys. Rev. A* **1988**, *38*, 3098 – 3100.
[33] J. P. Perdew, *Phys. Rev. B* **1986**, *33*, 8822 – 8824.
[34] J. Tao, J. P. Perdew, V. N. Staroverov, G. E. Scuseria, *Phys. Rev. Lett.* **2003**, *91*, 146401.
[35] E. J. Baerends, D. E. Ellis, P. Ros, *Chem. Phys.* **1973**, *2*, 41.
[36] B. I. Dunlap, J. W. D. Connolly, J. R. Sabin, *J. Chem. Phys.* **1979**, *71*, 3396.
[37] A. Schäfer, C. Huber, R. Ahlrichs, *J. Chem. Phys.* **1994**, *100*, 5829 – 5835.
[38] G. Schaftenaar, J. H. Noordik, *J. Comput.-Aided Mol. Des.* **2000**, *14*, 233 – 242.

Received: May 11, 2015
Revised: September 11, 2015
Published online on October 16, 2015

